AIAA JOURNAL
Vol. 31, No. 11, November 1993

Three-Dimensional Navier-Stokes Analysis of Tip Clearance Flow in Linear Turbine Cascades

Jong-Shang Liu* and Riccardo Bozzola†
Textron Lycoming Turbine Engine Division, Stratford, Connecticut 06497

A three-dimensional viscous flow code was used to study the tip clearance flow in linear turbine cascades. Two test cases with detailed measurements were used for validation. The flow properties inside the tip gap, such as static pressure, velocity, and angle, were compared with the data. The blade loading at different span locations and the downstream flowfield properties, such as loss and angle, were also compared with the data. The clearance flow phenomena, such as leakage vortex, changing of loss distribution, and flow underturning, were predicted by the numerical code. This code not only can be used as an analysis tool to study tip clearance effects in real turbine blade rows but also can be used as a design tool to design the turbine components.

Introduction

THE effort expended to develop a modern gas turbine engine is substantial. A significant portion of this effort is devoted to the preliminary design of aerodynamic components and subsequent modification by iteration to achieve the final design that meets the required engine performance goals. With the rapid growth in computer technology, computational fluid dynamics (CFD) codes are used as an analysis tool to help engineers understand the flow features in turbine components. Use of CFD codes that can accurately predict operation characteristics of turbomachinery components will result in considerable reduction of development effort and provide increased performance.

The validation of a CFD code is necessary to use it as a design tool. To evaluate the performance of the CFD code, reliable experimental data are needed. The data should provide detailed information for flow features in turbine components.

Unshrouded turbine rotors operate with a tip clearance between the blade tip and the casing. The fluid that leaks between the blade tip and casing causes large efficiency losses. The tip leakage flow also changes the loss distribution, exit flow angle, and loading. Therefore, it is important for the turbomachinery designer to understand and predict the tip clearance flow phenomena.

Hah,[1] Pouagare and Delaney,[2] and Dawes[3] predicted tip clearance flow using a three-dimensional Navier-Stokes code; however, all compressor blade rows are calculated with the assumption of zero thickness on the blade tip. They used one grid line and periodic conditions for the flow inside the tip clearance region. This model is satisfactory for very thin airfoils, such as those found at the tip of a transonic compressor rotor. However, thick airfoils, found in turbine blades, require the full flowfield resolution in the tip gap region. Moore and Moore[4] predicted the tip clearance flow in a linear turbine cascade with the three-dimensional incompressible Navier-Stokes code. However, the flow in turbomachinery components is usually compressible. In this study, a numerical code that solves three-dimensional, compressible Navier-Stokes equations was modified for validation purposes to calculate linear cascade test cases with tip clearance. A computational grid was modified to contain several grid points in the tangential direction within the tip gap region. This captured the tip clearance flow features for thick turbine blades. The code validation was carried out by a detailed comparison with experimental data from two linear turbine cascade test cases, Moore and Moore[4] and Yaras and Sjolander.[5] The comparisons between the computed results and experimental data included important design features such as exit total pressure and flow angle, plus the flow properties inside the tip clearance region, such as velocity, angle, and pressure. This code can accurately predict the tip clearance flow characteristics and can be used as an accurate and cost-effective design tool.

Numerical Analysis

An in-house three-dimensional viscous flow code, developed by Subramanian and Bozzola[6] for solving the turbomachinery flowfield, was used for the study of the tip clearance effects on the blade rows. This code solves the Reynolds-averaged, time-dependent, three-dimensional, Navier-Stokes equations in stationary or rotating cylindrical coordinates. The Baldwin-Lomax eddy viscosity model[7] was incorporated into this code. The numerical scheme is based on the explicit, four-stage, Runge-Kutta scheme originally proposed by Jameson and Baker.[8] This code has been successfully run for a variety of compressor and turbine cascades with and without tip clearance, and the predictions are in very good agreement with available test data.[9,10]

This code was extended to include a tip clearance model for thick blades by Liu et al.[10] and was modified to calculate linear cascade test cases with tip clearance for validation purposes in this study. The governing equations were converted from cylindrical coordinates to Cartesian coordinates, and four types of boundary conditions were used: inlet, exit, periodic, and wall boundary conditions. At the inlet, the total pressure, total temperature, and flow angle were specified. Static pressure was determined from left-running Riemann invariant or extrapolation from the interior. At the exit, a constant static pressure was specified through the whole span for calculating linear cascade test cases. The other variables were extrapolated from the interior. For the cells adjacent to solid boundaries, such as the blade surface, blade tip, hub wall, and casing, a zero flux condition was imposed. The wall static pressure was calculated by using the normal momentum equation. The no-slip condition was specified on the wall. The casing was a fixed wall or a moving wall to simulate the rotating condition. The periodic boundaries were treated as interior points in the calculation.

Received Nov. 1, 1992; presented as Paper 93-0391 at the AIAA 31st Aerospace Sciences Meeting, Reno, NV, Jan. 11-14, 1993; revision received March 20, 1993; accepted for publication March 20, 1993.

*Senior Development Engineer, Turbine Aero/Thermo Dynamics Department, 500 Main Street. Member AIAA.

†Manager, Aero/Thermo Dynamics Department, 500 Main Street.

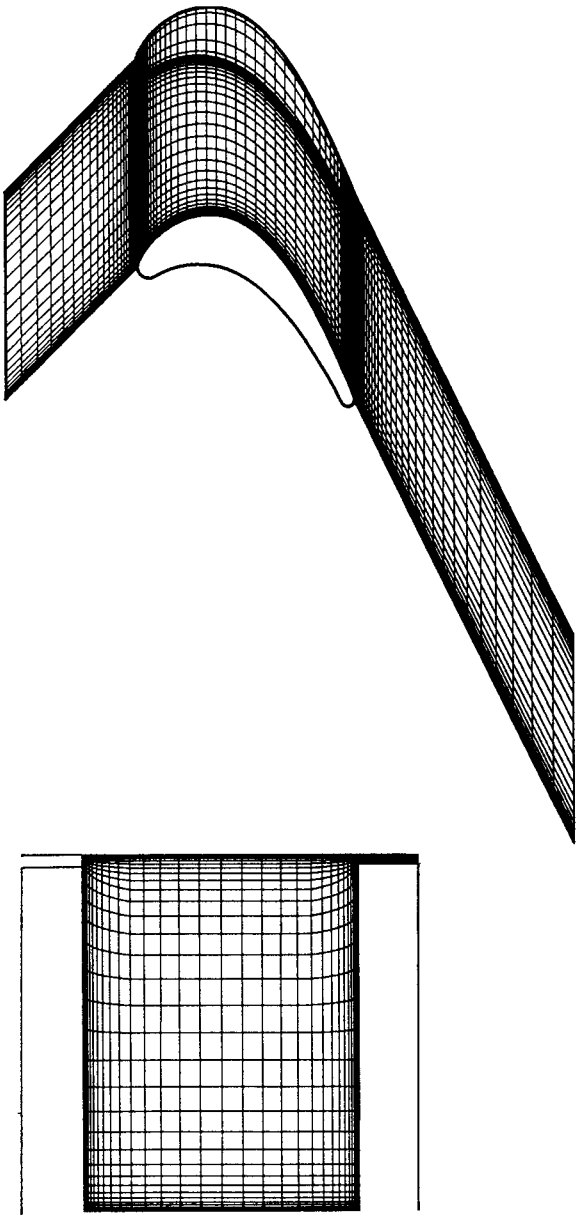

Fig. 1 Computational grid for VPI&SUcascade.

Results and Discussion

VPI&SUCascade

The first test case is a cascade tested at Virginia Polytechnic Institute and State University (VPI&SU) by Moore and Moore.[4] This is a large-scale cascade with a tip gap of 2.1% of blade height. The blade geometry is similar to Langston's cascade[11] and is a reaction turbine rotor section with 109-deg turning. The cascade has an aspect ratio of 1. Detailed information about this cascade geometry can be seen in Moore and Ransmayr.[12] The test flow through the cascade is incompressible, with the Reynolds number of 4.5×10^5 based on blade axial chord and exit velocity. The analytical simulation was conducted at the same Reynolds number level but at a higher Mach number level to improve solution accuracy (computation exit Mach = 0.28 vs experimental exit Mach = 0.1).

The computational grid of $31 \times 95 \times 31$ nodes in pitchwise, streamwise, and spanwise directions, respectively, used for calculation, is shown in Fig. 1. It is a simple sheared H-grid with an additional seven grid cells in the tangential direction and eight grid cells in the radial direction within the tip clearance region. It has 44 grid points between the blade leading and trailing edges. The grid was compacted around the leading and trailing edges and refined in a radial direction near the blade tip to capture the tip leakage flow features. The grid inside the tip clearance region is exponentially stretched in the tangential direction and is uniform in the radial direction.

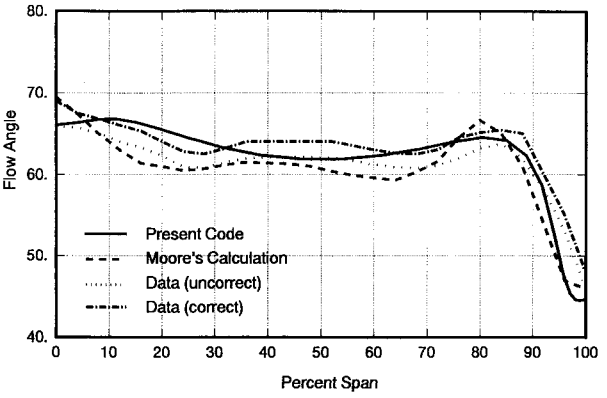

Fig. 2 Exit flow angle distribution.

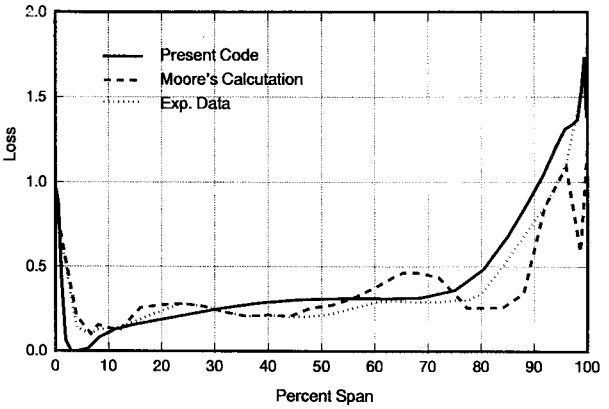

Fig. 3 Exit total pressure loss coefficient distribution.

The tangentially mass-averaged exit flow angle, at 40% of the axial chord downstream of the blade trailing edge, is shown in Fig. 2, where the computed results are compared with experimental data. The flow angle was defined as

$$\theta = 90 - \tan^{-1} \frac{\int_0^{\Delta y} \rho V_n V_x \, dy}{\int_0^{\Delta y} -\rho V_n V_y \, dy}$$

where x is the axial direction, y is the pitchwise direction, ρ is the density, V is the velocity, and Δy is the blade pitch. The experimental data are represented by two curves, the corrected and the uncorrected measurements. The uncorrected data are the data as taken from the measurements, and the corrected data curve is a distribution corrected in an attempt to allow the data to satisfy overall continuity. The present computed exit angle is between the two data curves, and the difference is less than 2 deg. The flow underturning near the tip end wall, due to the leakage flow, is shown clearly in this figure. Moore's computational results are also included in this figure for comparison. It can be seen that Moore's results agree better with the uncorrected data. The exit total pressure loss coefficient at the same plane is given in Fig. 3. The total pressure loss coefficient was defined as

$$C_{pta} = \frac{\int_0^{\Delta y} \rho V_n C_{pt} \, dy}{\frac{1}{\Delta z} \int_0^{\Delta x} \int_0^{\Delta y} \rho V_n \, dy \, dz}$$

where $C_{pt} = (P_{t0} - P_t)/(\frac{1}{2}\rho U_0^2)$, P_t is the total pressure, P_{t0} is the cascade inlet total pressure, U_0 is the cascade inlet freestream velocity, Δy is the blade pitch, and Δz is the passage height. The data and calculated results are in good agreement in the region between 10 and 75% span. In the near tip region, where losses caused by leakage flow are concentrated, the present calculation predicts higher loss than measured.

The velocity vectors on the blade-to-blade surface near the tip endwall are presented in Fig. 4. This figure shows how the flow leaking through the tip clearance gap moves away from the blade suction surface. This leakage flow interacts with the overturned endwall flow near the suction surface and rolls down from the endwall to form a leakage vortex. The endwall flow visualization from measurements included in this figure shows similar leakage flow features. The limiting streamline from the present computation at the same plane is given in Fig. 5. The flow splits when approaching the leading edge. It flows either to the suction side of the blade as the familiar overturning of the endwall flow or across the gap from the pressure side to the suction side of the next blade as it merges with the endwall flow from the next passage forming the leakage vortex. The three-dimensional view of the particle trace shows the leakage flow is given in Fig. 6. The flow through the tip gap forms the leakage vortex near the pressure surface as shown clearly in this figure. Figure 7 shows the inlet and exit velocity vectors at the midheight of the tip gap. There is little change in the flow direction from the pressure side to suction side, except near the blade leading edge. The flow direction is almost perpendicular to the airfoil camber line.

The accumulated flow through the tip gap exit nondimensionalized by mass flux through the passage vs axial distance along the blade is given in Fig. 8. The present calculations show smaller mass flux across the tip gap after 75% axial chord. Predicted and measured blade loading distribution at

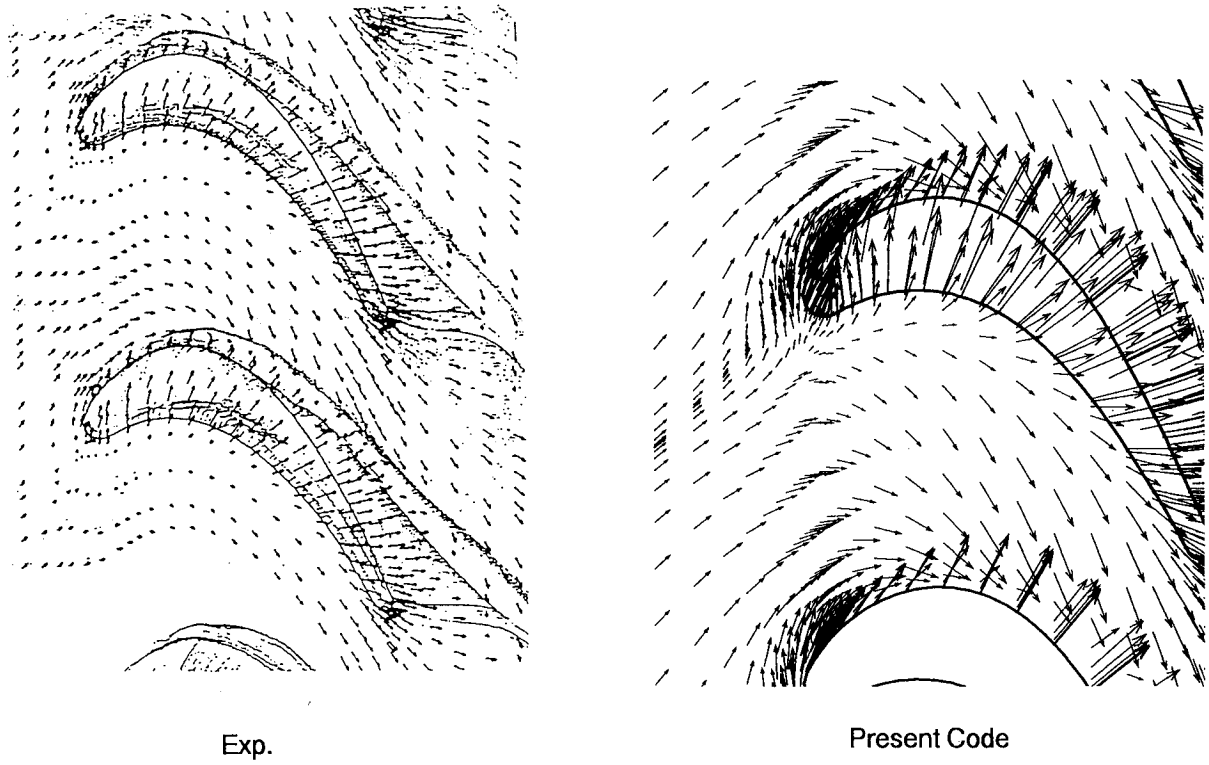

Fig. 4 Velocity vectors at near tip endwall, experiment and present code.

Fig. 5 Limiting streamline at near tip endwall.

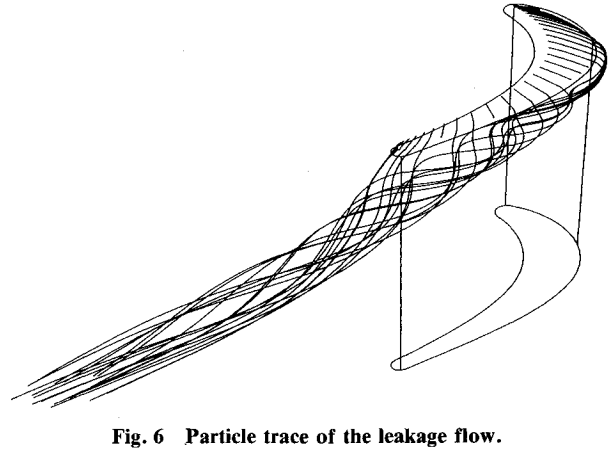

Fig. 6 Particle trace of the leakage flow.

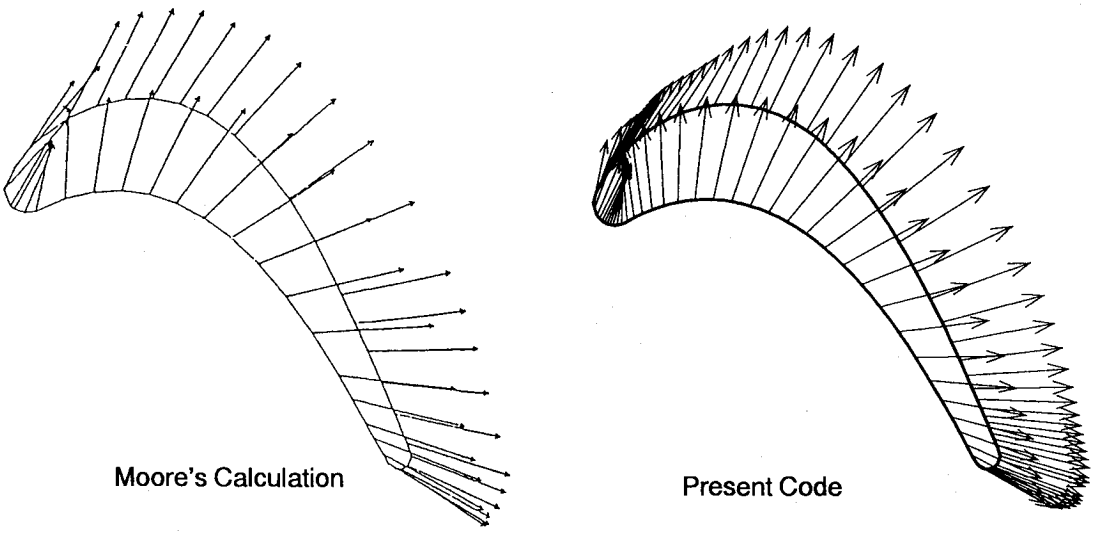

Fig. 7 Inlet and exit velocity vectors at midheight of the tip gap, Moore's calculation and present code.

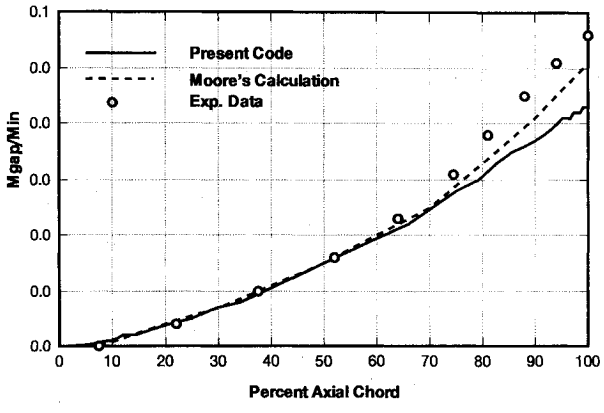

Fig. 8 Accumulated flow through the tip gap exit.

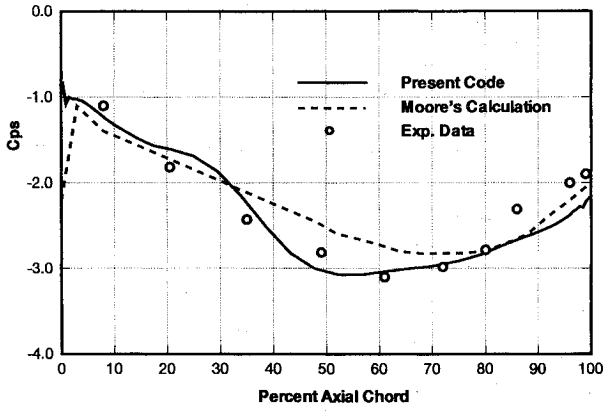

Fig. 10 Static pressure coefficient distribution at the tip gap exit on the endwall.

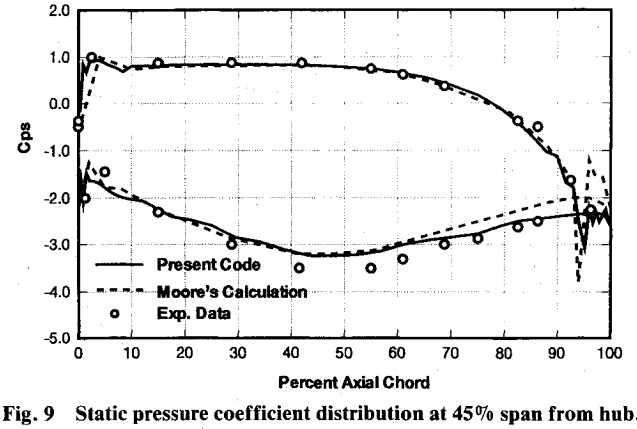

Fig. 9 Static pressure coefficient distribution at 45% span from hub.

45% span from the hub is shown in Fig. 9. The calculated pressures agree well on the pressure side with the experimental data; however, there are discrepancies between the predicted and measured values on the suction side from 30 to 70% axial chord. This is probably due to the inadequate grid resolution in that region. The static pressure distribution at the tip gap exit on the endwall is shown in Fig. 10. It can be seen in this figure that the agreement between the calculated and experimental data is very good. Based on the previous comparisons, it can be concluded that the present code can model the overall flow development in this turbine cascade with tip clearance, including loss distribution, flow turning, surface pressure distribution, and tip clearance flow structures.

Carleton Cascade

The second test case is Sjolander's cascade, designed and tested at Carleton University in Canada. It is a linear turbine cascade with an aspect ratio of 0.8. The detailed information about the cascade geometry can be found in Sjolander and Amrud.[13] The test conditions and the experimental results were given in Ref. 5. Detailed measurements were made inside the tip gap. The clearance of 3.2% of the blade chord, which is 3.9% of the blade span, was computed and compared with data. The measurement was obtained at a Reynolds number of 4.3×10^5, based on the blade chord and the undisturbed upstream velocity. The computation was conducted at the same Reynolds number but at a higher Mach number for accuracy. Both rotated and nonrotated blade test cases were calculated in this study. Rotation was simulated by using moving tip casing walls as the boundary conditions. This is the same as simulating rotation experimentally by using a moving belt tip wall.[14,15]

The grid refinement study was carried out for this test case. The baseline grid, grid 1, contains $31 \times 95 \times 31$ grid points in pitchwise, streamwise, and spanwise directions, respectively. It has 8 grid cells in both tangential and radial directions in the tip clearance region and 44 grid points between the blade leading and trailing edges. Grid 2 has 46 nodes in the radial direction and the same nodes in the pitchwise and streamwise directions as in grid 1. This grid contains 12 grid cells in the radial direction in the tip clearance region. Grid 3 has $31 \times 122 \times 31$ grid points. It has 70 points between the blade leading and trailing edges.

For simplicity, the moving tip casing wall calculation was only carried out for grid 1. The flow properties inside the tip gap, comparing the computed and experimental results, are presented first. The chordwise distribution of the velocity, nondimensionalized by inlet velocity, flow angle, and the static pressure coefficient at midgap height, are shown in Figs. 11, 12, and 13, respectively. The data were from the fixed wall experiments, whereas the computed results with and without a moving tip wall are included. The speed of the moving wall is set at 2.17 times the inlet velocity, as suggested in Ref. 14. The computational results on all three computational grids show similar results. The flow properties do not show grid-independent solutions in the tip clearance region. However, all three grids capture the basic flow structures. In general, the computed results are in good agreement with the measurements.

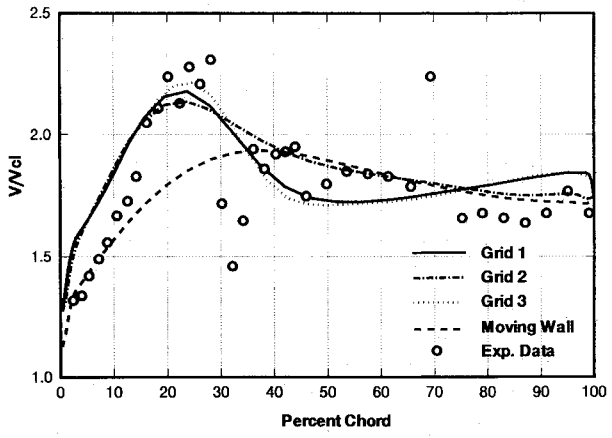

Fig. 11 Tip gap velocity distribution.

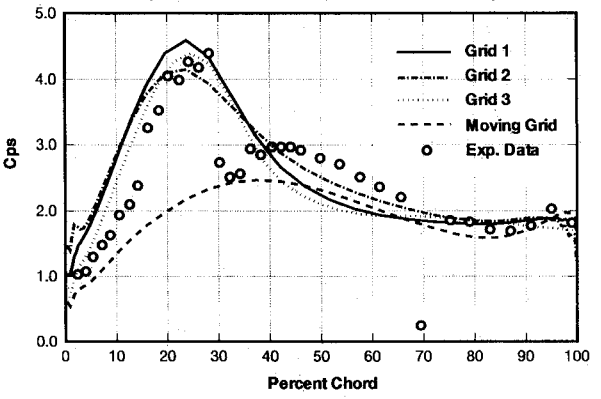

Fig. 13 Tip gap static pressure distribution.

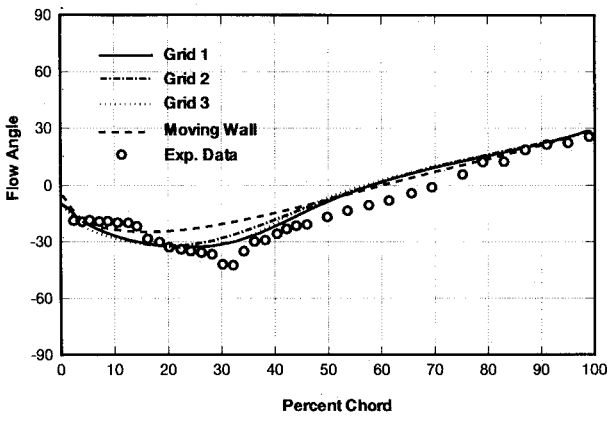

Fig. 12 Tip gap flow angle distribution.

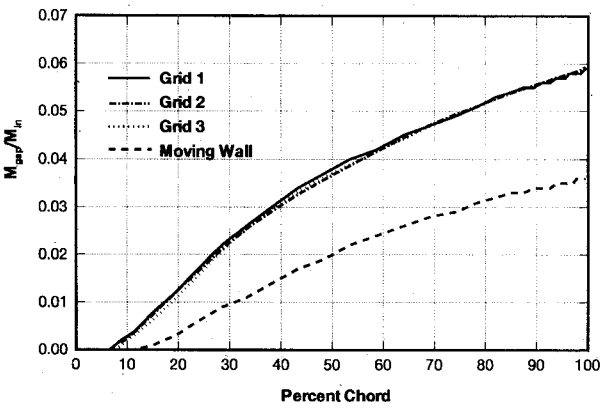

Fig. 14 Accumulated flow through the tip gap exit.

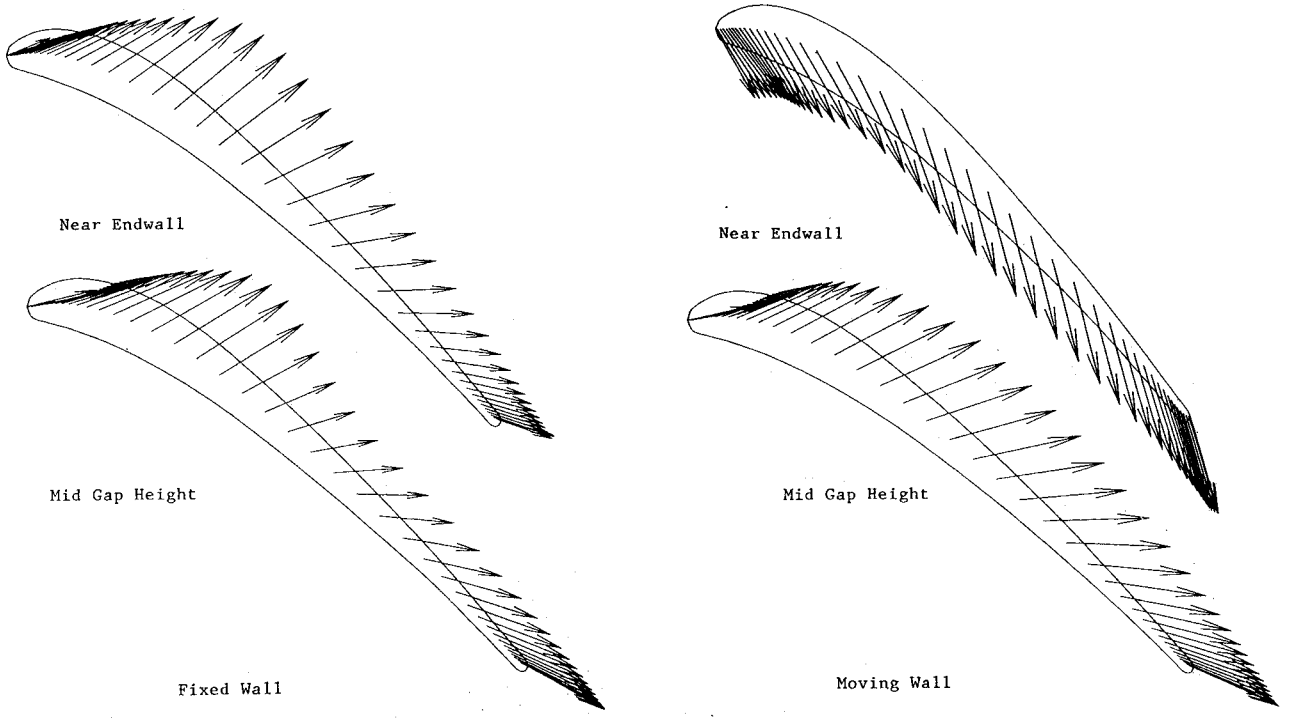

Fig. 15 Tip gap velocity vectors, fixed and moving walls.

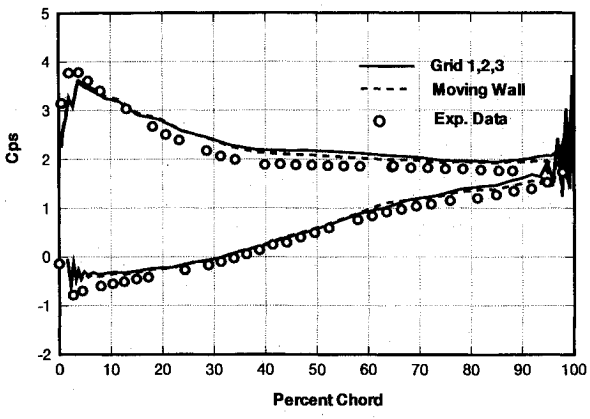

Fig. 16 Static pressure distribution at midspan.

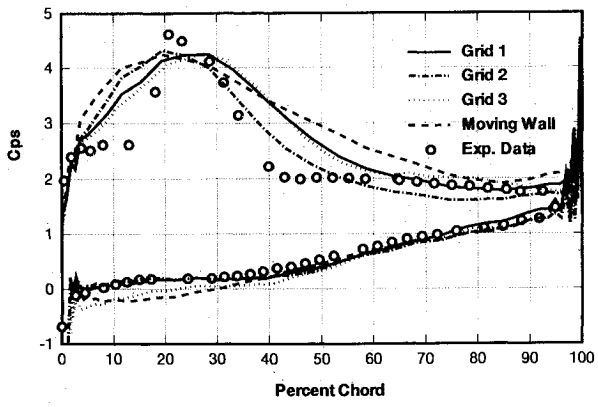

Fig. 17 Static pressure distribution at 2.12% span from blade tip.

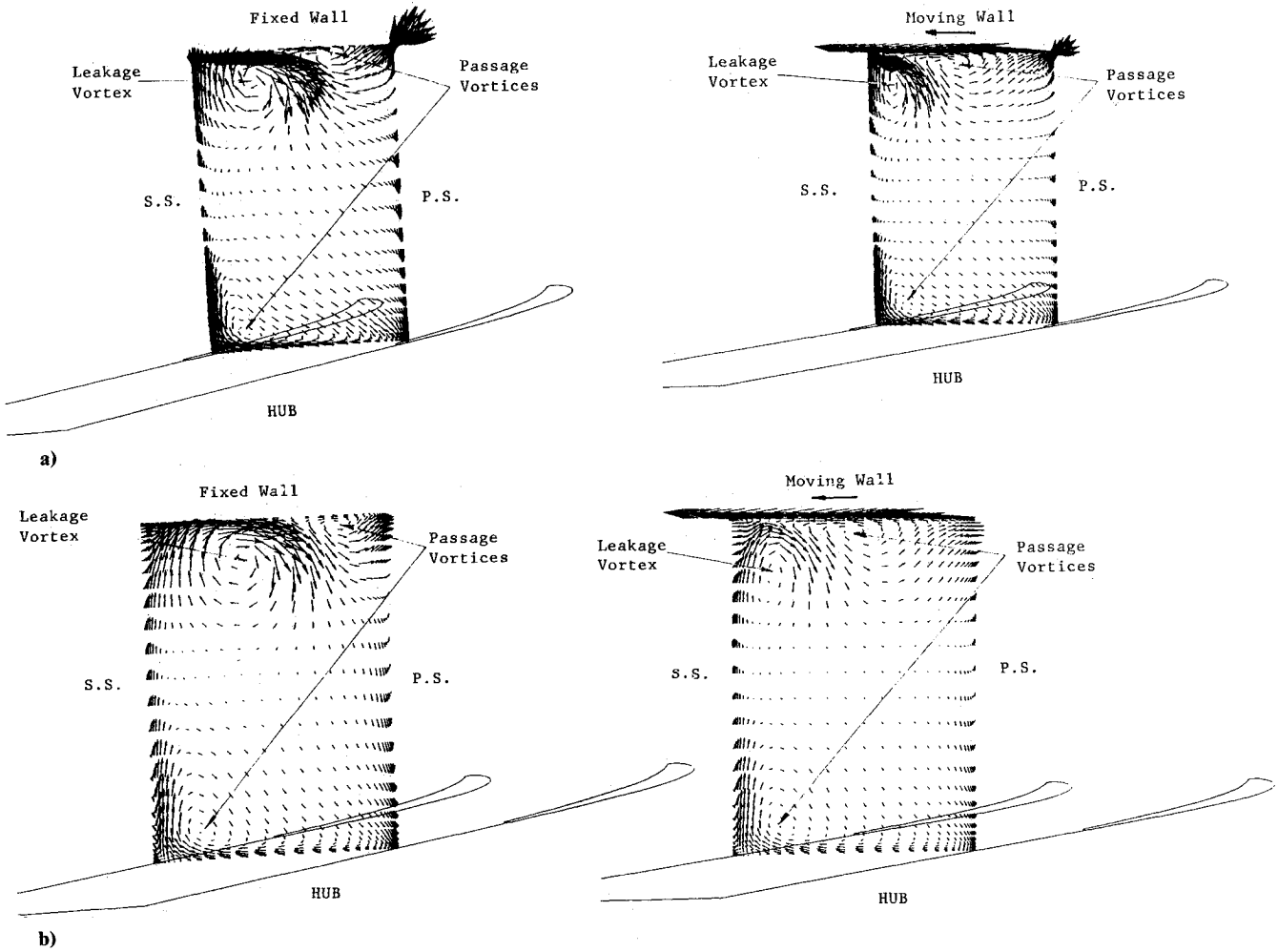

Fig. 18 Secondary velocity vectors: a) 5% upstream of the trailing edge and b) 40% downstream of the trailing edge.

The major discrepancy between the computational results and the data is at the 30% chord. The data show that the gap velocity, angle, and pressure all have a sharp drop or discontinuity. This may be because of the inaccuracy of the experiment or because the computational grid in that region is not fine enough to capture the sharp drop. With the moving tip wall, the gap velocity decreases in comparison with the fixed wall case. This may be because the viscous force on the wall drags the gap flow from pressure side to suction side, or it may be the result of the pressure difference between the pressure and suction sides decreasing, which reduces the driving force.

The computed accumulated gap exit mass flux, nondimensionalized by the inlet mass flux, vs percent chord for the fixed and moving wall cases is given in Fig. 14. The results from three different grids are almost identical. The reduction of the gap exit mass flux by the moving wall model is evident in this figure. This is consistent with the velocity vectors shown in Fig. 12, since with the moving wall the velocity inside the gap drops, which reduces the mass flux across the tip gap. The computed velocity vectors inside the tip gap at midgap height and near the tip casing are shown in Fig. 15. The flow leaks from the pressure side to suction side at midgap height can be clearly seen from this figure. Near the tip casing, where the viscous force dominates, the fluid flows in the same direction as the moving wall. This is in the opposite direction of the flow for the fixed wall case.

The static pressure distribution on the blade surface at midspan is given in Fig. 16. Identical results were obtained for

three different grids. The computed results and data are in good agreement. The moving wall has almost no influence on the pressure at midspan. The static pressure distribution on the blade surface at 2.12% span from blade tip is shown in Fig. 17. On the pressure side, the effects of the leakage flow are minor and the pressure distribution is similar to that at midspan. However, the pressure distribution on the suction surface changes dramatically near the blade tip. The suction peak is at 20% chord and is stronger than that at midspan. This is attributable to the tip vortex effects according to Yaras and Sjolander.[15] The discrepancy between the predicted and measured pressure between 40 and 50% chord is again probably due to the grid resolution.

The computed secondary velocity vectors for the crossflow plane, viewed from downstream to upstream along the axial line at approximately 5% axial chord upstream of the blade trailing edge and 40% axial chord downstream of the blade trailing edge, are shown in Fig. 18. The secondary velocity is defined here as the velocity component perpendicular to the primary flow direction, which is assumed to coincide with the streamwise grid line direction. The development of the leakage vortex is evident in this figure. Downstream, the passage vortex on the lower half of the span has already rolled to the suction side of the blade. With the moving wall, the passage vortex of the upper half of the span moves to the suction side, blocks the leakage vortex, and reduces the strength and size of the leakage vortex. According to Yaras and Sjolander,[15] this blockage seems to raise the pressure at the gap outlet, thereby reducing the driving pressure difference for the leakage flow and the mass flux leakage through the tip gap.

Summary

A three-dimensional, Navier-Stokes, turbomachinery code was modified to analyze a linear cascade with tip clearance. The rotation of the blade was simulated by using the moving tip casing wall boundary condition. Two test cases, with and without the moving walls, were presented in this study. Detailed comparisons were made with the computational results and measured data. The tip clearance flow structures, leakage vortex, flow underturning, and the effect of the tip clearance on blade loading and losses were predicted by the computer code. The predictions are in good agreement with the experimental data. The grid refinement study shows that the code needs more grid points in the tip clearance region. Yet it has been shown that the current grid density is sufficient to capture the basic flow features. This investigation shows that this code can be used as an analysis tool to help designers understand the tip clearance flow features.

Acknowledgments

This research was conducted as part of Textron Lycoming's Independent Research and Development program. The authors would like to thank Textron Lycoming management for supporting this research and permitting the presentation of these results. The authors would also like to thank S. A. Sjolander of Carleton University for providing the information regarding the tip-leakage experiments.

References

[1]Hah, C., "A Numerical Modeling of Endwall and Tip-Clearance Flow of an Isolated Compressor Rotor," American Society of Mechanical Engineers, ASME Paper 85-GT-116, March 1985.

[2]Pouagare, M., and Delaney, R. A., "Study of Three-Dimensional Viscous Flows in an Axial Compressor Cascade Including Tip Leakage Effects Using a SIMPLE-Based Algorithm," American Society of Mechanical Engineers, ASME Paper 86-GT-84, June 1986.

[3]Dawes, W. N., "A Numerical Analysis of the Three-Dimensional Viscous Flow in a Transonic Compressor Rotor and Comparison with Experiment," *Journal of Turbomachinery,* Vol. 109, No. 1, 1987, pp. 83–90.

[4]Moore J., and Moore, J. J., "A Computational Study of Tip Leakage Flow and Losses in a Linear Turbine Cascade," AGARD-CPP-510, May 1991.

[5]Yaras, M. I., and Sjolander, S. A., "Measurement of the Tip Clearance Flow in a Rectilinear Cascade of Turbine Blades: A Test Case for Computational Methods," Dept. of Mechanical and Aeronautical Engineering, Carleton Univ., Rept. M&AE 88-1, Ottawa, Ontario, Canada, April 1988.

[6]Subramanian, S. V., and Bozzola, R., "Numerical Simulation of Three-Dimensional Flow Fields in Turbomachinery Blade Rows Using the Compressible Navier-Stokes Equations," AIAA Paper 87-1314, June 1987.

[7]Baldwin, B., and Lomax, H., "Thin Layer Approximation and Algebraic Model for Separated Turbulent Flows," AIAA Paper 78-257, Jan. 1978.

[8]Jameson, A., and Baker, T. J., "Multigrid Solution of the Euler Equations for Aircraft Configurations," AIAA Paper 84-0093, Jan. 1984.

[9]Subramanian, S. V., "Three-Dimensional Multigrid Navier-Stokes Computations for Turbomachinery Applications," AIAA Paper 89-2453, July 1989.

[10]Liu, J. S., Minkkinen, G., and Bozzola, R., "Analytical and Experimental Determination of Tip Clearance Effects in a High Work Turbine Rotor," American Society of Mechanical Engineers, ASME Paper 91-GT-197, June 1991.

[11]Langston, L. S., Nice, M. L., and Hooper, R. W., "Three-Dimensional Flow Within a Turbine Cascade Passage," *ASME Journal of Engineering for Power,* Vol. 99, No. 1, Jan. 1977, pp. 21–28.

[12]Moore, J., and Ransmayr, A., "Flow in a Turbine Cascade: Part I—Losses and Leading-Edge Effects," *Journal of Engineering for Gas Turbine and Power,* Vol. 106, No. 2, 1984, pp. 400–408.

[13]Sjolander, S. A., and Amrud, K. K., "Effects of Tip Clearance on Blade Loading in a Planar Cascade of Turbine Blades," *Transactions of the ASME, Journal of Turbomachinery,* Vol. 109, No. 2, 1987, pp. 237–245.

[14]Yaras, M. I., and Sjolander, S. A., "Effects of Simulated Rotation on Tip Leakage in a Planar Cascade of Turbine Blades, Part I: Tip Gap Flow," American Society of Mechanical Engineers, ASME Paper 91-GT-127, June 1991.

[15]Yaras, M. I., and Sjolander, S. A., "Effects of Simulated Rotation on Tip Leakage in a Planar Cascade of Turbine Blades, Part II: Downstream Flow Field and Blade Loading," American Society of Mechanical Engineers, ASME Paper 91-GT-128, June 1991.